Ultrathin Silicon Membranes for Wearable Dialysis

Dean G. Johnson, Tejas S. Khire, Yekaterina L. Lyubarskaya, Karl J. P. Smith, Jon-Paul S. DesOrmeaux, Jeremy G. Taylor, Thomas R. Gaborski, Alexander A. Shestopalov, Christopher C. Striemer, and James L. McGrath

The development of wearable or implantable technologies that replace center-based hemodialysis (HD) hold promise to improve outcomes and quality of life for patients with ESRD. A prerequisite for these technologies is the development of highly efficient membranes that can achieve high toxin clearance in small-device formats. Here we examine the application of the porous nanocrystalline silicon (pnc-Si) to HD. pnc-Si is a molecularly thin nanoporous membrane material that is orders of magnitude more permeable than conventional HD membranes. Material developments have allowed us to dramatically increase the amount of active membrane available for dialysis on pnc-Si chips. By controlling pore sizes during manufacturing, pnc-Si membranes can be engineered to pass middle-molecular-weight protein toxins while retaining albumin, mimicking the healthy kidney. A microfluidic dialysis device developed with pnc-Si achieves urea clearance rates that confirm that the membrane offers no resistance to urea passage. Finally, surface modifications with thin hydrophilic coatings are shown to block cell and protein adhesion.

Key Words: Biocompatible materials, Biocompatibility testing, Hemodialysis, Microfluidic devices, Nanopores

Introduction

End-stage renal disease (ESRD) affects 2 million people worldwide,[1] and this population has been growing at a rate greater than 8%.[2] In the United States in 2010, nearly 600,000 patients received renal replacement therapy, almost 400,000 of which underwent dialysis.[3] The standard of care for ESRD, when kidney transplantation is not available or feasible, is lifelong hemodialysis (HD) treatments at a frequency of 3 to 4 times per week. Even with frequent HD, the life expectancies for ESRD patients aged 30 to 85 years are typically less than 10.5 years.[4] In an effort to improve the access to dialysis and the quality of life for those on renal replacement therapy, research groups, including ours, are working on technologies for wearable HD.[5-7] These advances would not only provide lifestyle benefits of mobility and convenience, but they could also improve outcomes by reducing extracorporeal blood volumes and enabling more frequent or continuous dialysis.

A prerequisite for wearable HD technology is the development of highly efficient membranes that can achieve standard toxic clearance rates with far less membrane. Clinical HD currently uses membranes that are approximately 10 μm thick with tortuous flow paths. These characteristics slow diffusion and convection through membranes; consequently, dialyzers have long flow channels (15-18 in.) and large membrane surface areas (1.4-2.4 m^2) to achieve target clearance values. The extended extracorporeal circulation increases the risk of hemolysis,[8] the breakdown of red blood cells, and thrombus formation.[9] Thus, shorter dialysis flow paths not only enable portability, but they also have the potential to ameliorate other complications. Current work on wearable HD devices has focused on miniaturization of the fluidics, controls, and improved membrane selectivity,[10] but it has not addressed the need for increased membrane efficiency.

Here we report on the application of porous nanocrystalline silicon (pnc-Si) membranes for inclusion in a small-format HD device. These membranes, which were first described by our group 6 years ago,[11] are 100 to 1000 times thinner than conventional membranes and are therefore orders of magnitude more efficient for dialysis.[12] In fact, given the molecular thickness of these membranes (~15 nm) and their appreciable porosity (~15%), pnc-Si membranes operate near the maximum permeability that is achievable for a nanoporous membrane. In addition, the membrane pore sizes can be tuned to match specific molecular separation goals,[13] and the silicon platform allows for scalable manufacturing and straightforward integration with fluidics. We report on material advancements that have allowed us to make pnc-Si membranes with 26-fold more active membrane area than previously possible. We describe the design and operation of a benchtop microfluidic system that achieves target urea dialysis goals predicted from finite-element models of our system. We also examine the use of surface functionalization to reduce protein and cellular attachment to pnc-Si and render the membranes hemocompatible.[14]

From Department of Biomedical Engineering, University of Rochester, Rochester, NY.

T.R.G., C.C.S., and J.L.M. are co-founders of SiMPore Inc., a commercial manufacturer of ultrathin silicon membranes.

Address correspondence to Dean G. Johnson, PhD, Biomedical Engineering, University of Rochester, Robert B. Goergen Hall, Room 318, Box 270168, Rochester, NY 14627. E-mail: deangjohnson@rochester.edu

1548-5595/$36.00

http://dx.doi.org/10.1053/j.ackd.2013.08.001

Material and Methods

High-Area pnc-Si Membranes

The fabrication of pnc-Si membranes has been previously described in detail.[12,13] In brief, the membrane material is formed by annealing an ultrathin layer of amorphous silicon deposited on a silicon wafer by sputter deposition. Annealing creates nanocrystals and adjacent nanopores that span the thickness of the annealed layer. Annealing temperature, layer thickness, substrate bias, and other fabrication parameters are used to control pore sizes. The membrane is made freestanding by chemical etching through the backside of the supporting wafer. This etching process naturally creates channels that conform to the area of the freestanding membrane.

The separation characteristics of membranes with average pore sizes between 10 and 30 nm were examined for the ability to separate bovine serum albumin (BSA; molecular weight [MW] = 66 kD) from β2-microglobulin (β2M; MW = 12 kD), the largest protein toxin in HD. We used cytochrome c (MW = 12 kD) as a surrogate for β2M because the molecule's strong visible absorbance at 415 nm facilitates detection in the presence of albumin. We examined the ability of the membranes to separate cytochrome c and BSA using diffusion-based separations[12] and centrifuge-based separations.[15] Cytochrome c concentrations were 1 mg/mL and BSA concentrations were 1.33 mg/mL in phosphate-buffered saline (PBS). Cytochrome c and BSA were purchased from Sigma-Aldrich (St. Louis, MO).

To increase the freestanding area of membranes while maintaining mechanical integrity, we developed a silicon nitride (SiN)-based support scaffold (Fig 1). Our technique involved the use of low-pressure chemical vapor deposition to place a 400-nm-thick low-stress (250 MPa) SiN layer above the amorphous silicon layer. We used standard photolithography to pattern tessellated hexagons with 42-μm openings and 5-μm-wide frames. Reactive ion etching was used to transfer the photopattern into the nitride, and the silicon dioxide (SiO_2) layer above the pnc-Si[11,12] served as an etch stop. The resulting support structure reduces the effective porosity of the hybrid membrane by only approximately 12%.

CLINICAL SUMMARY

- pnc-Si membranes provide unprecedented permeability that is needed for small-format HD.
- Membranes can be engineered to pass middle-molecular-weight toxins and urea while retaining albumin.
- Microfluidic dialysis devices made with pnc-Si achieve target urea clearance rates.
- Hydrophilic molecules can be grafted to pnc-Si surfaces to promote hemocompatibility.

Single-Channel Dialysis Device

Single-channel devices were created by incorporating fluidic components formed in polydimethylsiloxane (PDMS) with 11- by 20- mm membrane chips (Fig 2A) in the test fixture. The test fixture consisted of two acrylic plates that are used to clamp the flow channels to the hybrid membrane (Fig 2D). The fluidic channel on the backside of the etched silicon is bounded by pnc-Si/SiN hybrid membrane on one side and the cap of PDMS on the other side (Fig 2C). The flow channels, inlet/outlet, were fabricated with the Sylgard 184 PDMS (Dow Corning, Midland, MI) patterned and cured on a custom-ordered SU-8 mold with a feature height of 300 μm (Stanford Microfluidics Foundry, Stanford, CA). Holes for the inlets and outlets were punched into the cured PDMS using a blunt 20-gauge needle (Small Parts, Inc., Logansport, IN). Glass microcapillaries with inner/outer diameter of 500 μm/900 μm (Friedrich & Dimmock, Inc., Millville, NJ) were cut into shorter segments and inserted into the punched holes in the flow compartment as the adaptors for tubing attachment. Tygon tubing with inner/outer diameter of 1/32 in./3/32 in. (Saint-Gobain Performance Plastics Corporation) were used to connect the glass microcapillaries to the syringe and the fraction collector.

Multichannel Dialysis Device

Multichannel devices were constructed in a similar fashion as single-channel devices, only the membrane chips were 22 × 24 mm with 13 parallel microfluidic channels (Fig 2B). An important consideration for the multichannel device was the design of a fluid bus that distributes flow evenly across all 13 channels. The bus system was designed with the use of a finite-element model of our systems (COMSOL Multiphysics, Stockholm, Sweden). Figure 3A illustrates that a shallow straight bus (height = 100 μm) results in a flow rate that is much higher in the central channels near the input than at the periphery. Using a flow rate of 5.6 μL/minute in each channel, we found that uniform flow can be achieved using a thin bus that expands gradually from the source or by increasing the height of a straight bus bar. For example, using a bus bar height of 300 μm, simulations showed a flow of 5.6 μL/minute in all channels with less than a 1% deviation (Fig 3B). We fabricated a fluidic chip with a 300-μm deep bus bar and visualized

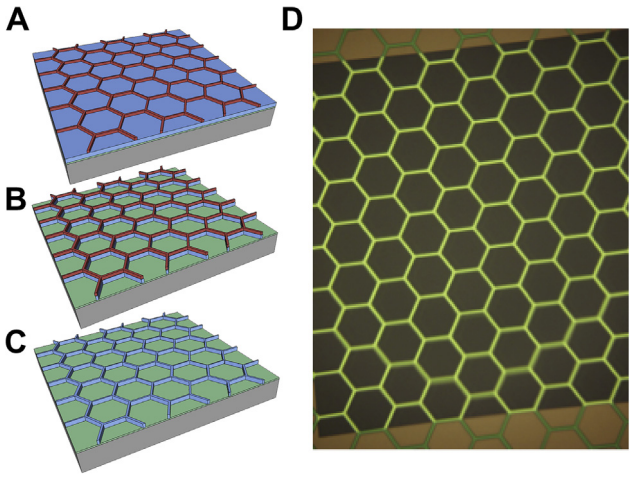

Figure 1. Silicon nitride scaffolding fabrication process. A silicon substrate with a 20-nm-thick silicon nanomembrane is coated with a 400-nm-thick LCPVD nitride. (A) The wafer is spin coated with PR, which is patterned with the scaffolding structure. (B) A reactive ion etch is used to transfer the photopattern of the PR to the nitride. (C) The PR is removed, via plasma etching, leaving the patterned silicon nitride scaffolding on top of the membrane material. (D) Micrograph of silicon nitride scaffolding supporting the silicon nanomembrane. The scaffolding is a repeating pattern of hexagons with 5-μm-wide supports. The width of the hexagons is 82 μm. The porosity of the scaffolding is ~90%. Abbreviations: LCPVD, low-pressure chemical vapor deposition; PR, photoresist.

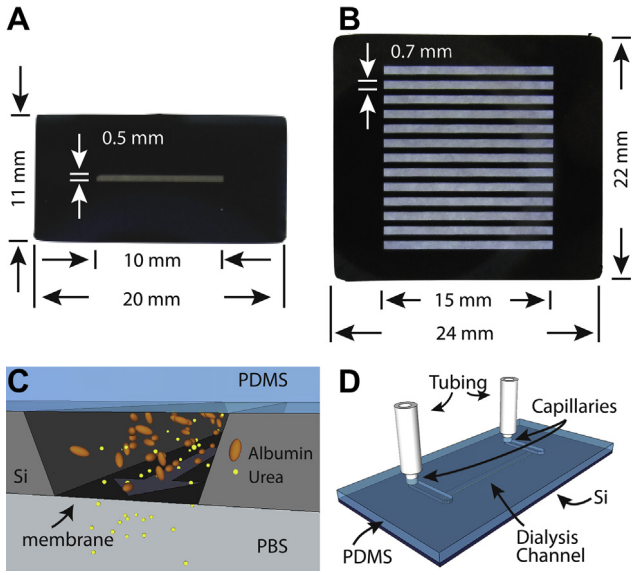

Figure 2. Single-channel and multichannel dialysis chips. (A) Single-slot dialysis chip used for conducting urea dialysis tests. The channels are 500 μm wide on the membrane side and 10 mm long. (B) Multichannel dialysis chips. Multichannel dialysis chip (22 × 24 mm) with 13 parallel dialysis channels. The channels are 700 μm wide and 15 mm long on the membrane side. (C) Cross-sectional drawing of a membrane chip in use shows how the channel etched through the silicon becomes a microfluidic channel with the nanomembrane as a boundary. (D) 3-Dimensional drawing of single-slot dialysis test device. Flexible tubing (1 mm inner diameter) connects to glass capillaries inserted into PDMS cap with channels connecting to a fluidic channel in the bulk silicon over silicon nanomembrane. Abbreviations: PBS, phosphate-buffered saline; PDMS, polydimethylsiloxane.

water flow with dye (Fig 3C). Experimental tests verified a relatively uniform dye front across all 13 channels.

Urea Dialysis Studies

Solutions containing urea and fetal bovine serum (FBS) were pumped through single-channel devices to measure the urea dialysis rate in the presence of a complex protein background. The inlet port was connected to a syringe pump with a 10-mL syringe filled with a solution of 0.5 mM urea in 30% FBS and 70% PBS. Keeping serum at levels below 50% allowed us to neglect the effect of viscosity on fluid flow and diffusion while still presenting a complex protein environment to the membrane.[16] The syringe pump moved the solution through the single slot dialysis chip, which was suspended in a stirred beaker of 100% PBS exposing the backside of the membrane to a vigorously stirred beaker containing 100% PBS. Dialyzed samples were collected with a fraction collector that switched collection vials every 30 minutes. The experiment was conducted for over 30 hours pumping at a rate of 5.6 μL/minute. Experiments were performed at 4°C to minimize evaporation of the collected samples. Urea concentrations in collected fractions were measured by absorbance using a urea assay kit as described by the manufacturer (Abcam, Cambridge, MA). The membranes used in these experiments were not functionalized to prevent fouling. This was done to collect baseline data on the untreated membranes. Once the static functionalization studies have been completed, additional experiments will be run with modified membrane surfaces to show the effects, if any, of the functionalization on long-term clearance.

Dialysis experiments were done with and without priming of the device and degassing of solutions. Priming was performed by first wetting the nanomembrane with isopropanol and drawing additional isopropanol through the channel filling the tubing connected to the inlet port. A syringe was filled with degassed PBS and pumped through the device for more than 1 day before the introduction of serum and urea. In this manner, the isopropanol was chased with more than 4000 volumes of PBS and should have had no residual effects when protein is introduced. The FBS/PBS solution for this experiment was also degassed before pumping through the device.

Urea clearance rates are calculated with the following expression[17]:

$$K = (Q_I C_I - Q_O C_O)/C_I$$

C_I and C_O are the concentration of solute in the blood at the input and output, respectively, of the dialyzer. Q_I and Q_O are the flow rates at the input and output,

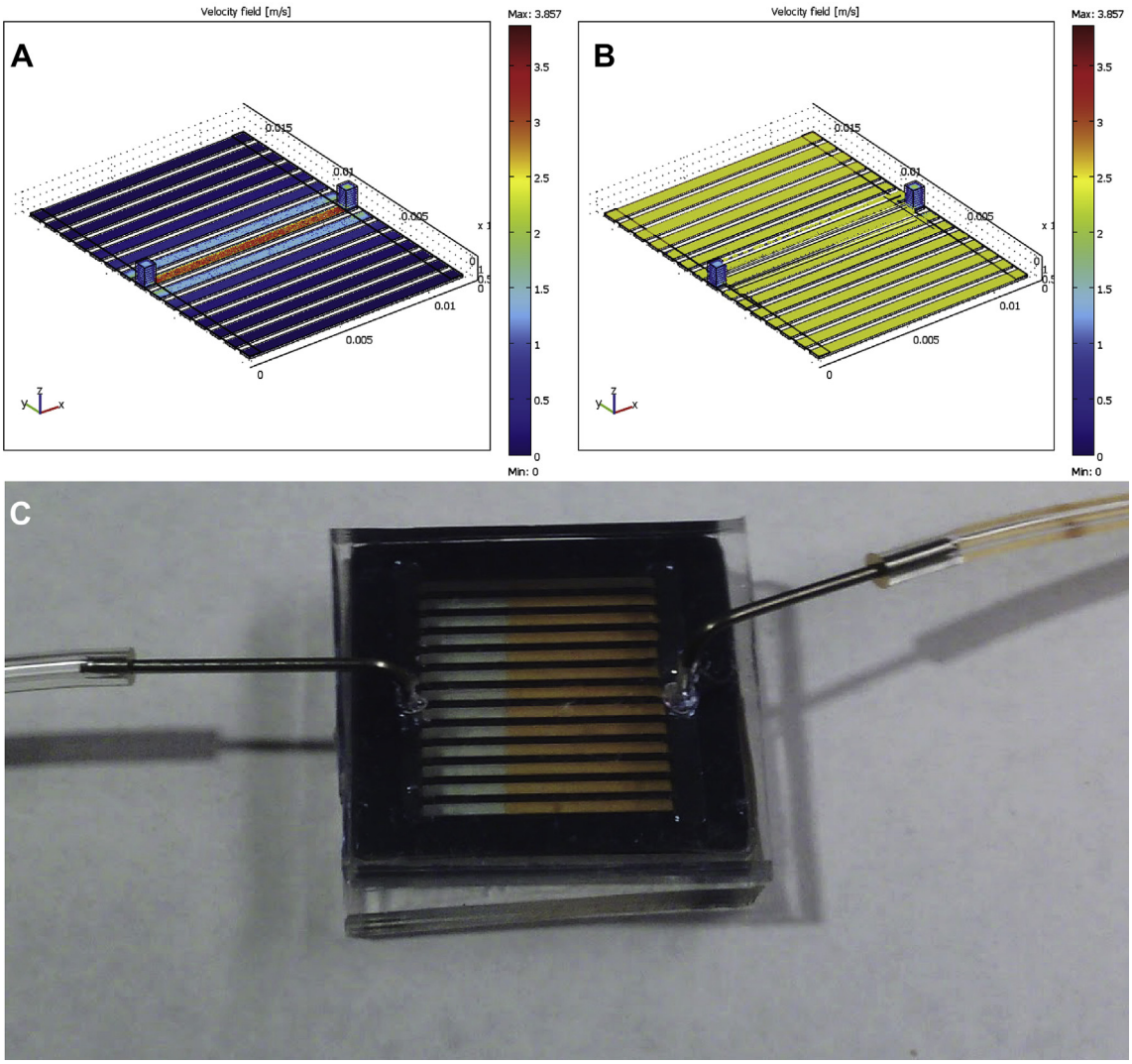

Figure 3. Design of multichannel dialysis fluidics. Inlet and outlet connect to a single fluidic bus delivering fluid to the individual dialysis channels. (A) COMSOL model with 100-μm-deep fluidic bus bar. Velocity field indicates that flow will move more quickly down the center channel and have nearly zero flow along the outboard channels. (B) COMSOL model with 300-μm-deep fluidic bus bar shows even flow across all microchannels. The large volume of the bus bar allows for even fluid flow to all of the channels. (C) Image of 300-μm bus bar fabricated with silicone gasket and PDMS cap shows nearly even flow in all microchannels as predicted by the model. Abbreviation: PDMS, polydimethylsiloxane.

respectively. Because our dialysis systems are open and the pressure in the beaker is lower than the pressure in the channel, the exit flow rate is lower than the input flow rate as urea is removed by convection through the membrane (ultrafiltration) in addition to diffusion-based dialysis. Another metric for evaluating the dialysis membrane is the instantaneous urea dialysis rate.

The instantaneous urea dialysis rate is defined as

$$R = 1 - C_O/C_I$$

Because ultrafiltration through the membrane removes urea and fluid at the same rate, it does not lower the sample concentration. Thus the instantaneous urea dialysis rate only measures the effectiveness of the diffusive component of urea removal.

A finite-element convection/diffusion model was developed to guide the device design and predict urea dialysis rates. The model was developed with COMSOL with the addition of the microfluidics module. For urea dialysis studies with single-channel devices as shown in Figure 1, the COMSOL simulation considers a structure with a single rectangular channel with inlet and outlet ports. The channels are 300 μm tall, 500 μm wide, and 10 mm long. Counterflow through the underlying dialysate chamber is configured to mimic the conditions in a stirred beaker. The starting point for the COMSOL model was the 2-dimensional equations for flow and diffusion in a rectangular channel. We assumed the stirred beaker, with a volume of 250 mL, would act as a perfect sink for the urea diffusion for the 5 mL of 0.5-mM urea. The COMSOL model was tuned by adjusting

the dialysate flow until it matched the results of the 2-dimensional analytical solution. Urea diffusion was considered to take place at the rate of free diffusion.[12]

Surface Functionalization

Protein and cellular binding has the potential to trigger immune or coagulation cascades. Therefore, we, as Muthusubramaniam and colleagues[14] before us, are investigating the potential of short hydrophilic molecules to block protein and cellular adhesion to silicon membranes. Successful attempts to make inert surfaces with polyethylene glycol (PEG) polymer brushes[18] are not appropriate because the 50- to 100-nm-thick coatings will occlude pores. Thus, our objective is to establish coatings that are much smaller than pore sizes yet still prevent biological adhesion. We compared our own methods for grafting short PEG (6- to 10-mer) to silicon at high density[19] with the proprietary approach of a local diagnostics device manufacturer (Adarza Biosystems, Inc., West Henrietta, NY) and tested for protein and cellular binding.

We compared 2 chemical modifications of the silicon surface to reduce nonspecific protein binding. In the first approach, we contracted Adarza Biosystems, Inc., to vapor deposit a proprietary monolayer silane (sLink) to create an amine-reactive surface that was subsequently reacted with (9- to 12-mer) amino-terminated PEG or ethylamine (EA). The amino-PEG molecules were reacted with activated membranes in toluene or dichloromethane, and EA reactions were performed entirely in the vapor phase.

Second, we used our own procedures for creating highly stable PEG linkages by replacing unstable silicon-oxygen bonds with silicon-carbon bonds. First, oxide-free silicon was created and subsequently reacted to yield an inert methyl-terminated primary layer. A secondary layer was attached to the primary monolayer via carbene insertion to yield stable carbon-carbon bonds. This overlayer comprises densely spaced *N* -hydroxysuccinimide esters that can react with amine-terminated molecules.[19] Specifically, we used a liquid-based reaction of either 2 or 4 mmol dodecaoxaheptatriacontane (m-dPEG$_{12}$-amine; Quanta Biodesign Limited) to yield the desired PEG overlayer.

Protein Adhesion

To test the ability of surface functionalization to prevent protein and cell adhesion, we fabricated "windowless" 1- by 1-cm membrane chips. These chips were formed without performing a backside etch through the supporting silicon; therefore, they have identical surfaces to dialysis chips. This format was designed to simplify handling because drying steps can fracture membranes on standard chips.

After a prewetting rinse in PBS, test chips were incubated with 5 mg/mL fluorescein-conjugated BSA in PBS in a humidified chamber for 12 hours at 4°C. The samples were rinsed in PBS and then deionized water, and then they were dried with filtered, compressed air. Measurements were taken with a Zeiss Axiovert fluorescent microscope (Romulus, MI) and analyzed with ImageJ (http://rsbweb.nih.gov/ij/) for image intensity. Background measurements were determined from untreated chips and subtracted from sample data. The background signal subtracted is an order of magnitude lower than the signal from the positive control, ensuring that we are not significantly underestimating protein binding.

Platelet Activation and Adhesion

Platelet-rich plasma (PRP) was collected from healthy donors following established protocols.[20] Platelet activation and adhesion protocols largely followed those of Muthusubramaniam and colleagues[14] but are detailed here for accuracy. PRP (200 μL) was dispensed on membrane chips with or without prior oxygen-plasma treatment or onto control surfaces for 2 hours at 37°C. Adenosine diphosphate (ADP; Sigma Aldrich), a calcium stimulator, was used as a positive control for platelet activation. ADP was reconstituted in PBS and added to a final concentration of 40 μM. Teflon was chosen as a negative control because of its ability to repel protein and cell binding. Glass cover slips were used as a positive control. The PRP was incubated on test surfaces for 2 hours at 37°C. The surfaces were removed from PRP, rinsed gently by dipping in PBS, and then fixed with 4% paraformaldehyde for 15 minutes followed by 1% BSA blocking for 30 minutes. The surfaces were again washed with PBS to remove unabsorbed BSA molecules. Test surfaces were incubated with antihuman CD62 P (P-selectin) mouse monoclonal antibody for 1 hour followed by Alexa Fluor 546 donkey anti-mouse secondary antibody for another hour. Lastly, the surfaces were incubated with antihuman CD41 FITC-conjugated mouse monoclonal antibody diluted 300× for 1 hour. The surfaces were washed with PBS after every labeling step to avoid any nonspecific binding. Finally, the surfaces were imaged under an inverted fluorescent microscope to assess any platelet adhesion (green channel) and/or platelet activation (red channel). All antibodies were purchased from Life Technologies (Grand Island, NY).

Results

Membrane Selectivity

We investigated the ability of functionalized pnc-Si membranes to fractionate a binary protein mixture consisting of 12-kD cytochrome c and 66-kD BSA. In this test, cytochrome c is used as a surrogate for β2M. β2M is among the largest molecules cleared by the healthy kidney and a source of joint discomfort and possible osteoarthropathy in long-term HD patients.[21] Cytochrome c is a useful

surrogate for β2M because its strong absorbance at 415 nm allows it to be easily distinguished from albumin when used in a binary mixture.

We tested pnc-Si membranes that had been functionalized with EA with average pore diameters between 10 and 20 nm for the ability to fractionate solutions of cytochrome c and BSA using diffusion[12] and pressurized flow[15] as transport modes. We found that membranes with a cutoff at the low end of this range (Fig 4) exhibited the desired separation characteristics in both modes. Although the membrane pore sizes are far larger than the molecular sizes of cytochrome c (~2.4 nm) and BSA (~6.8 nm), we have consistently found that electrostatic interactions and protein adsorption reduce the effective pore sizes of pnc-Si membranes compared with pore sizes measured by electron microscopy.[12,15]

Figure 4C shows a sodium dodecyl sulfate–polyacrylamide gel electrophoresis gel displaying the results of a diffusion experiment in which a small-pore membrane transmits monomeric cytochrome c and retains albumin and dimeric cytochrome c. Sodium dodecyl sulfate-resistant dimeric cytochrome c is a known contaminant in commercial cytochrome c because of its tendency to aggregate during detergent-based purification.[22] Here, the dimeric contaminant provides a useful measure of the resolution of pnc-Si, indicating the ability of the membranes to discriminate between monomeric and dimeric cytochrome c.

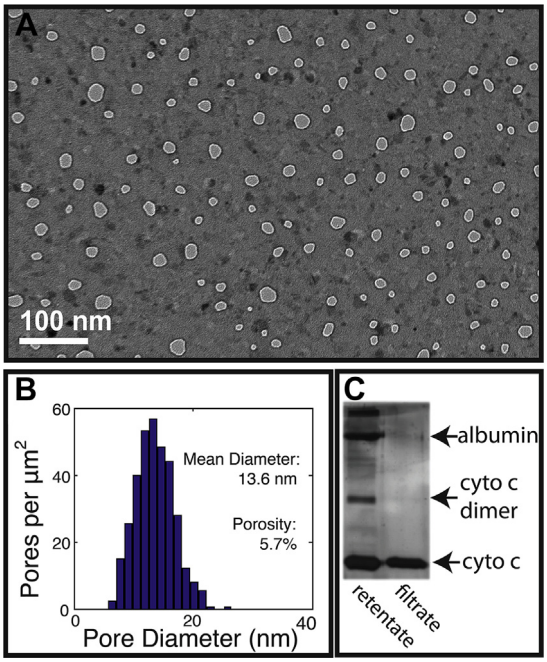

Figure 4. Membrane selection. (A) Transmission electron microscope image of ultrathin porous silicon nanomembrane. Light areas are pores. (B) Histogram of pore diameter (nm) of the membrane. The mean pore diameter is 13.6 nm and the porosity is 5.7%. The sharp cutoff of the histogram allows for high-resolution separations. (C) Image of sodium dodecyl sulfate-polyacrylamide gel showing that the cytochrome c passes from the retentate through the membrane to the filtrate whereas the membrane holds back the albumin and even the cytochrome c dimer.

Urea Dialysis

We assessed the ability of pnc-Si membranes to dialyze urea at rates predicted by a COMSOL-based convection-diffusion model that assumes uninhibited diffusion of urea through the membrane.[12] Negligible resistance to diffusion of toxins is the key to enabling high clearance rates in portable devices. Simulations were configured to match the physical dimensions of single-channel dialysis chips (Fig 2) with flow rates of 5.6 μL/minute.

The urea dialysis test was performed in a case in which we first primed the channel with isopropanol and PBS flushes of the system to ensure proper wetting and in a case in which we did not. Without priming we found that urea dialysis values included episodes of near-zero urea dialysis, which we assume were due to incomplete wetting of the membrane[23] and/or trapping of gas bubbles beneath the membrane. With priming and degassing, we found that the exit concentration initially falls short of the predicted value ($C_O = 0.34$ mM) and then settles to this value over a day of continuous use. Thus, instead of finding that membrane fouling slowed urea dialysis with time, the dialysis rate actually improved. Our current hypothesis is that ultrafiltration (passage of fluid by convection through the membrane) slows as serum protein adsorbs to the membrane over time; thus, transport occurs more by pure diffusion as assumed in the COMSOL model. On the basis of recovered volumes after the experiments, we know that approximately 17% of the volume entering the membrane passes through by ultrafiltration.

Cell and Protein Binding to Native and Modified Membranes

Although day-long exposure to 30% serum did not block membrane pores in our urea dialysis studies, the time-dependent behavior we observed is clearly undesirable. For this reason and to prevent immune or coagulation cascades, we are investigating the potential of short hydrophilic molecules to block protein and cellular adhesion to silicon membranes. Figure 5A shows the results of our protein binding studies. In these experiments, fluorescent-tagged BSA was incubated with membrane chips in a humidified chamber for 12 hours at 4°C and binding was assessed by fluorescence microscopy. All surface chemistries reduced protein binding to less than 5% of untreated controls. Higher concentrations of amine-reactive PEG yielded slight improvements for the in-house reactions whereas dichloromethane gave slightly better results than toluene when used as a solvent. The most impressive results were obtained for EA, which leaves the surface with only a terminal hydroxyl group connected to the surface through a diamine linkage.

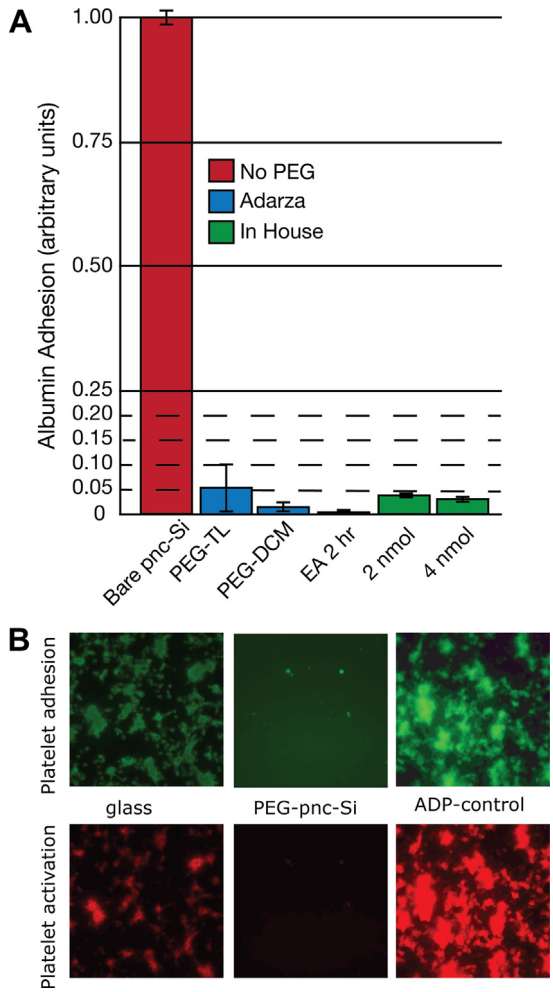

Figure 5. Protein and cell adhesion on functionalized membranes. (A) Fluorescence of absorbed protein normalized to bare pnc-Si. All treatments reduce protein binding to more than 5% of control. (B) Platelets are double-labeled with platelet marker (CD41 in green) and activated platelet marker (CD62 P in red). ADP is used as a positive control to induce platelet activation and aggregation. PEG treatment significantly reduces platelet binding and activation. Abbreviations: ADP, adenosine diphosphate; DCM, dichloromethane; EA, ethylamine; PEG, polyethylene glycol; pnc-Si, porous nanocrystalline silicon; TL, toluene.

Because of the small size of EA (~1 nm), the entire process is done in vapor phase and likely has the highest density of any of our test surfaces. However, the temporal stability of this chemistry will need to be tested because we have generally found that vapor-based processes produce less stable coatings than liquid-based processes.

Using our in-house methods, we also examined the ability of PEG-coatings to reduce platelet adhesion and activation. Cells were incubated with test surfaces for 2 hours at 37°C before being fixed, labeled, and imaged by fluorescence microscopy. Platelets were double-labeled with a general platelet marker (CD41) and activated platelet marker (CD62 P), and ADP was used as a positive control that promoted adhesion and activation. As seen in Figure 5B, PEG treatment significantly reduced platelet adhesion and activation compared with uncoated surfaces and glass.

Discussion

The development of silicon-based membranes for the bioartificial kidney (BAK) has been a focus of the pioneering efforts of Roy, Fissell, and colleagues.[10,14,24,25] Although many system components must come together to make the BAK a reality,[26] a highly efficient membrane platform is fundamental. Assuming membrane pore sizes are fixed to give molecular discrimination that mimics the healthy kidney, only the porosity and the thickness of a membrane can be adjusted to improve membrane permeability. Thus, as molecularly thin nanoporous membranes with porosities that can approach approximately 20%,[27] the silicon nanomembranes we are developing operate close to the maximum permeability that can be achieved for a passive HD membrane. Our report demonstrates (1) the ability to manufacture nanomembranes with appropriate separation characteristics, (2) the capacity to modify these membranes to improve hemocompatibility, and (3) the ability to integrate into dialysis devices that achieve predicted urea dialysis rates after a day of use. It is important to note that the predicted dialysis rates assume the membrane offers no resistance to the diffusion of urea, confirming the expectation of ultrahigh efficiency.

Typical ESRD patients experience the equivalent kidney urea clearance of approximately 30 mL/minute for a 4-hour period 3 times in a week at dialysis centers. Our goal is a device that achieves this level of total clearance in a small format and at reasonable cost. Simulations suggest that the optimal clearance through the current 13-channel chip format is approximately 0.1 mL/minute (at total chip flow rate of ~0.45 mL/minute). Assuming daily dialysis for 10 hours, a device containing 50 chips would be needed to achieve the target weekly clearance. Although 50 chips could be packaged into a device the size of a modern smartphone, material costs would likely be prohibitive unless the membranes were to be used for months at a time. Further optimization of chip design, flow conditions, and manufacturing efficiency should achieve another 3-fold reduction in material requirements. Efforts to make mechanically stable freestanding sheets of nanomembrane (>10 cm^2) that would dramatically reduce cost are underway.

Despite the potential of ultrathin silicon nanomembranes, much work remains before the membranes will be used for HD. The most immediate need is the establishment of stable surface chemistries that give steady clearance of whole blood for days without activating plasma or immune systems. The design and assembly of a multichip device is an engineering challenge that lies ahead. The focus of our efforts is a small-format

device for toxin clearance. Integration of this as a module in a complete treatment device that addresses vascular access, toxin trapping, electrolyte balance, glucose balance, and ultrafiltration will benefit from the considerable efforts of others to make the BAK a reality.

Acknowledgments

This research was funded by Coulter Foundation Award #002773. The authors thank Jess Snyder for her assistance with diffusion-based separation experiments.

References

1. Blagg CR. The 50th anniversary of long-term hemodialysis: University of Washington Hospital, March 9th, 1960. *J Nephrol.* 2011;24(Suppl 17):S84-S88. Italy.
2. Schieppati A, Remuzzi G. Chronic renal diseases as a public health problem: Epidemiology, social, and economic implications. *Kidney Int Suppl.* 2005;98:S7-S10.
3. U.S. Renal Data System. *USRDS 2012 Annual Data Report: Atlas of Chronic Kidney Disease and End-Stage Renal Disease in the United States*. Bethesda, MD: National Institute of Diabetes and Digestive and Kidney Diseases; 2012.
4. Turin TC, Tonelli M, Manns BJ, Ravani P, Ahmed SB, Hemmelgarn BR. Chronic kidney disease and life expectancy. *Nephrol Dial Transplant.* 2012;27:3182-3186.
5. Fissell WH, Roy S, Davenport A. Achieving more frequent and longer dialysis for the majority: Wearable dialysis and implantable artificial kidney devices. *Kidney Int.* 2013;84(2):256-264.
6. Lee DBN, Roberts M. Automated Wearable Artificial Kidney (AWAK): a peritoneal dialysis approach. In: *Proceedings of the World Congress on Medical Physics and Biomedical Engineering: Diagnostic and Therapeutic Instrumentation, Clinical Engineering*. 7th ed. Munich, Germany: Springer Verlag; 2009:104-107.
7. Gura V, Macy AS, Beizai M, Ezon C, Golper TA. Technical breakthroughs in the wearable artificial kidney (WAK). *Clin J Am Soc Nephrol.* 2009;4(9):1441-1448.
8. Vieira FU, Antunes N, Vieira RW, Alvares LM, Costa ET. Hemolysis in extracorporeal circulation: relationship between time and procedures. *Rev Bras Cir Cardiovasc.* 2012;27(4):535-541.
9. Cosemans JM, Angelillo-Scherrer A, Mattheij NJ, Heemskerk JW. The effects of arterial flow on platelet activation, thrombus growth, and stabilization. *Cardiovasc Res.* 2013;99(2):342-352.
10. Fissell WH, Dubnisheva A, Eldridge AN, Fleischman AJ, Zydney AL, Roy S. High-performance silicon nanopore hemofiltration membranes. *J Memb Sci.* 2009;326(1):58-63.
11. Striemer CC, Gaborski TR, McGrath JL, Fauchet PM. Charge- and size-based separation of macromolecules using ultrathin silicon membranes. *Nature.* 2007;445(7129):749-753.
12. Snyder JL, Clark A, Fang DZ, et al. An experimental and theoretical analysis of molecular separations by diffusion through ultrathin nanoporous membranes. *J Memb Sci.* 2011;369(1-2):119-129.
13. Fang DZ, Striemer CC, Gaborski TR, McGrath JL, Fauchet PM. Methods for controlling the pore properties of ultra-thin nanocrystalline silicon membranes. *J Phys Condens Matter.* 2010;22(45):454134.
14. Muthusubramaniam L, Lowe R, Fissell WH, et al. Hemocompatibility of silicon-based substrates for biomedical implant applications. *Ann Biomed Eng.* 2011;39(4):1296-1305.
15. Gaborski TR, Snyder JL, Striemer CC, et al. High-performance separation of nanoparticles with ultrathin porous nanocrystalline silicon membranes. *ACS Nano.* 2010;4(11):6973-6981.
16. Yadav S, Shire SJ, Kalonia DS. Viscosity analysis of high concentration bovine serum albumin aqueous solutions. *Pharm Res.* 2011;28(8):1973-1983.
17. Pisitkun T, Tiranathanagul K, Poulin S, et al. A practical tool for determining the adequacy of renal replacement therapy. *Contrib Nephrol.* 2004;144:329-349.
18. Hucknall A, Simnick A, Hill R, et al. Versatile synthesis and micropatterning of nonfouling polymer brushes on the wafer scale. *Biointerphases.* 2009;4:FA50-FA57.
19. Shestopalov AA, Morris CJ, Vogen BN, Hoertz A, Clark RL, Toone EJ. Soft-lithographic approach to functionalization and nanopatterning oxide-free silicon. *Langmuir.* 2011;27(10):6478-6485.
20. Landesberg R, Roy M, Glickman RS. Quantification of growth factor levels using a simplified method of platelet-rich plasma. *J Oral Maxillofac Surg.* 2000;58(3):297-300. discussion 300-301.
21. Ahrenholz PG, Winkler RE, Michelsen A, Lang DA, Bowry SK. Dialysis membrane-dependent removal of middle molecules during hemodiafiltration. *Clin Nephrol.* 2004;62(1):21-28.
22. Hirota S, Hattori Y, Nagao S, et al. Cytochrome c polymerization by successive domain swapping at the C-terminal. *Proc Natl Acad Sci U S A.* 2010;107(29):12854-12859.
23. Kim J, Shen M, Nioradze N, Amemiya S. Stabilizing nanometer scale tip-to-substrate gaps in scanning electrochemical microscopy using an isothermal chamber for thermal drift suppression. *Anal Chem.* 2012;84(8):3489-3492.
24. Fissell WH, Dyke DB, Weitzel WF, et al. Bioartificial kidney alters cytokine response and hemodynamics. *Blood Purif.* 2002;20(10):55-60.
25. Kanani DM, Fissell WH, Roy S, Dubnisheva A, Fleischman A, Zydney AL. Permeability- selectivity analysis for ultrafiltration: effect of pore geometry. *J Memb Sci.* 2010;349(1-2):405.
26. Humes HD, Buffington D, Westover AJ, Roy S, Fissell WH. The bioartificial kidney: current status and future promise. *Pediatr Nephrol.* 2013 Apr 26 [Epub ahead of print].
27. Kavalenka MN, Striemer CC, Fang DZ, Gaborski TR, McGrath JL, Fauchet PM. Ballistic and non-ballistic gas flow through ultrathin nanopores. *Nanotechnology.* 2012;23(14):145706.